Synthesis and Characterization of Al_2O_3 Coated Li/Mn-Rich $Li_{1.2}Mn_{0.54}Ni_{0.13}Co_{0.13}O_2$ Cathode Materials for Li-Ion Battery Application

Seipati Rasesemola[1], Rebecca Mhlongo[2] and Mesfin A. Kebede[3,*]

[1]*Department of Physics, Sefako Makgatho Health Science University, Medunsa, South Africa.*
[2]*Department of Physics, University of Limpopo, Polokwane, South Africa.*
[3]*Institute for Nanotechnology and Water Sustainability (iNanoWS), University of South Africa, Johannesburg, South Africa.*

ABSTRACT

Lithium-rich manganese-based cathode materials are considered to be promising cathode materials for lithium-ion batteries (LIBs). In this study, Al_2O_3-coated $Li_{1.2}Mn_{0.54}Ni_{0.13}Co_{0.13}O_2$ cathode materials were successfully prepared via the sol-gel method. X-ray diffraction (XRD), Raman spectroscopy, scanning electron microscopy (SEM) coupled with energy-dispersive X-ray spectroscopy (EDS), and battery testing were employed to examine the structural, molecular, morphological, and electrochemical properties of the material. The XRD spectra confirmed the presence of monoclinic Li_2MnO_3 and the Li-rich Mn-based layered oxide structure, with all major peaks attributed to the hexagonal structure with space group $R\bar{3}m$ phase. As expected, the electrochemical tests revealed that the uncoated samples, herein referred to as pristine $Li_{1.2}Mn_{0.54}Ni_{0.13}Co_{0.13}O_2$ cathodes, exhibit a higher discharge capacity of 185 mAh g^{-1} at a current density of 0.1C within a voltage range of 2.8–4.35V, as compared to 168 mAh g^{-1} reported in the Al_2O_3-coated $Li_{1.2}Mn_{0.54}Ni_{0.13}Co_{0.13}O_2$ material. However, the coated sample voltage degradation and both electrodes exhibited stable cyclic behavior with a capacity retention of approximately 96% over 100 cycles. These results suggest that Al_2O_3 surface modification may contribute to improved voltage stability, cycling stability and structural protection, although it introduces a reduction in initial discharge capacity. Further studies involving impedance spectroscopy and cyclic voltammetry are recommended to clarify the role of coating in charge-transfer and interfacial processes.

KEYWORDS

Lithium-ion batteries, Sol-gel method, $Li_{1.2}Mn_{0.54}Ni_{0.13}Co_{0.13}O_2$, Al_2O_3 coated-$Li_{1.2}Mn_{0.54}Ni_{0.13}Co_{0.13}O_2$, Li-rich MNCO cathode materials

Received: 10 March 2026 Revised: 3 July 2026 Accepted: 15 August 2026

INTRODUCTION

Energy storage devices have become an area of research interest globally. Researchers are extensively investigating ways of improving such devices to address the need for energy and complement existing solutions. Among those, lithium-ion batteries (LIBs) have emerged as the mainstream energy storage field. However, the current materials could not meet the increasing demands for high energy density, high stability, and fast charging. Therefore, it is crucial to explore new-types of cathode materials with higher energy density. To a great extent, the promotion of performance depends on cathode materials with high quality which are having high voltage and high specific capacity in lithium-ion batteries. Among them, Lithium-rich Manganese-based cathode materials, which can be expressed as (LRMOs), have attracted much attention with Li-rich Mn-based layered oxides regarded as a promising category of cathode materials. This is due to their high specific capacity based on joint anionic (oxygen) / cationic redox chemistry at high operating voltages, thus high energy density and low cost.[1-3]

Trends in research and development (R&D) of advanced cathode active materials featuring Li/Mn-rich chemistry have been informed by the tradeoffs associated with the Ni-rich and Co-based chemistries. On the one hand, the incorporation of excess Ni was desirable given it contributed to the high voltage performance of the material and enhanced Li^+ diffusion, partly due to the lower activation barrier (210 meV) for Li^+ migration coupled with the lesser electrostatic repulsion between Li^+/Ni^{2+} during the migration process.[4,5] This means the migration of Li^+ is enhanced within the proximity of the Ni^{2+} ions. On the downside, mixing Ni^{2+} into the Li^+ layer remains a challenge.[6] The Co^{3+} provides the prerequisite electrical conductivity and structural stability necessary for long-term performance.[7] However, Co-rich materials suffer from increased volume thickness (0.163 μm to 35 μm) during charge/discharge as noted by Luo et al.[8] and Zhang et al.[9]

In light of the challenges associated with Co and Ni-rich materials, the development of Li/Mn-rich cathode materials with a stable layered structure, suppressed O_2 evolution, and voltage fading remains a priority. The Li-rich and Mn-based cathode materials offer unique advantages including thermal stability and higher specific discharge capacities above 250 mAh g^{-1} even at elevated voltages (> 4V).[10] The discharge capacity of Li/Mn-rich cathode materials can be attributed to the unique crystal structure that integrates the rhombohedral $R\bar{3}m$ ($LiTMO_2$, where TM represents the transition metals Mn, Ni and Co) phases and monoclinic C2/m (Li_2MnO_3).[11] During cycling, a layered structure is developed as Li^+ ions partially substitute the transitional metal ions (Ni^{2+}, Co^{3+}, and Mn^{2+}) at the tetrahedral sites in the *c*-axis.[12] The $Ni^{2+} \rightarrow Ni^{3+/4+}$ and $Co^{3+} \rightarrow Co^{4+}$ cationic redox reactions yield approximately 170 mAh g^{-1} of discharge capacity,[13] and the additional ~50–100 mAh g^{-1} is drawn from the $O^{2-} \rightarrow O_2^{n-}$ anionic redox reactions in the bulk cathode active material at voltages above 4.5 vs Li^+/Li.[13-15] On the downside, the prolonged cycling of Li/Mn-rich cathodes results in oxygen evolution, layered to spinel transformation, and ultimately voltage fading. These drawbacks could be attributed to the activation of the Li_2MnO_3 phase at higher voltages (see Equations 1a and 1b),[16] which catalyzes the migration of transitional metals into the Li layer,[17] formation of redox inactive layer[18,19] and enhancement of local displacement and structural strain.[11] The migration of transitional metals is coupled with the loss of O^{2-} and Li^+ from the lattice. Since the O^{2-} and Li^+ loss is irreversible, voltage decay is inevitable.

$$Li_2MnO_3 \rightarrow Li_2O + MnO_2 \quad [1a]$$

$$MnO_2 + Li^+ + e^- \leftrightarrow LiMnO_2 \quad [1b]$$

Despite the shortcomings associated with the activation of the Li_2MnO_3 phase, the unlocking of MnO_2 is beneficial considering

*To whom correspondence should be addressed
Email: mesfiak@unisa.ac.za

ISSN 1996-840X Online / South African Chemical Institute / http://saci.co.za/journal
© The Author(s) Published under a Creative Commons Attribution 4.0 International Licence (CC BY 4.0)
https://doi.org/10.17159/0379-4350/2026/v80se1a25

it participates in the subsequent redox reactions and amplifies the discharge capacity.[3,20,21] Other challenges with Li/Mn-rich cathode materials include parasitic reactions between the electrode and electrolyte, which result in a detrimental effect of the degradation of the initial capacity during cycling. To overcome these limitations, several surface modification strategies have been investigated for Li-rich layered cathode materials such as Al_2O_3, ZrO_2, TiO_2, and Li_3PO_4 have been reported to improve interfacial stability by minimizing direct contact between the cathode surface and electrolyte, suppressing transition-metal dissolution, and reducing undesirable side reactions during cycling. Among these coatings, Al_2O_3 has attracted considerable attention owing to its chemical stability, low cost and ability to form a protective surface layer that mitigates electrolyte decomposition and structural degradation.[22,23] Recent studies have demonstrated that oxide coatings can effectively improve capacity retention, suppress surface reconstruction, and enhance the cycling stability of Li-rich layered oxide cathodes.[22,24,25] Furthermore, advances in surface engineering have highlighted the importance of protective coating layers in maintaining structural integrity and reducing interfacial degradation during prolonged electrochemical cycling.

Chen et al.[26] synthesized Li-rich manganese-based layered cathode $Li_{1.2}Mn_{0.54}Ni_{0.13}Co_{0.13}O_2$ by electrospinning and surface-coated with different amounts of amorphous Al_2O_3, and the results showed that Al_2O_3 coating can stabilize the interface between electrolyte and electrode materials, whereby the capacity retention increased from 78.3% to 97.6% after 90 cycles. Zhang et al.[27] synthesized $Li_{1.2}Ni_{0.13}Co_{0.13}Mn_{0.54}O_2$ cathode material by the sol-gel method, and Al_2O_3-coated $Li_{1.2}Ni_{0.13}Co_{0.13}Mn_{0.54}O_2$ by a facile wet chemical method, and their initial discharge capacity are 259.54 mAh g^{-1} and 257 mAh g^{-1}, respectively. However, their Coulombic efficiencies were 75.64% and 76.16 %, respectively. Although previous studies reported on different synthesis methods for $Li_{1.2}Ni_{0.13}Co_{0.13}Mn_{0.54}O_2$, Ma et al.[28] reported on different synthesis temperatures using the sol-gel method and observed different electrochemical performances, whereby 800 °C was the optimum temperature.

Although the beneficial effects of Al_2O_3 coatings on Li-rich cathode materials have been reported,[29,30] further studies are required to understand their influence on the structural and electrochemical behaviour of $Li_{1.2}Mn_{0.54}Ni_{0.13}Co_{0.13}O_2$ prepared using the sol-gel synthesis route. Therefore, this study investigates the effect of an Al_2O_3 surface coating on the battery cathode performance of $Li_{1.2}Mn_{0.54}Ni_{0.13}Co_{0.13}O_2$ cathode materials.

EXPERIMENTAL

Chemicals and reagents

All the chemicals and reagents used for this experiment were analytical grade and were utilized in sol-gel synthesis without further purification. The chemicals and reagents used are $LiNO_3$ (97%), $Ni(NO_3)_2.6H_2O$ (99.9%), $Co(NO_3)_2.6H_2O$ (99.0%), and $Mn(NO_3)_2.6H_2O$ (98.8%), and $C_9H_{21}O_3Al$ (98.8%). All aqueous solutions were prepared with deionized (DI) water.

Sol-Gel Synthesis

The stoichiometric amounts of Nickel nitrate, $Ni(NO_3)_2.6H_2O$ (99.9%), Cobalt nitrate $Co(NO_3)_2.6H_2O$ (99.0%), Manganese II nitrate hexahydrate $Mn(NO_3)_2.6H_2O$ (98.8%) and $LiNO_3$ (97%) were dissolved in deionized water (DI) to prepare the $Li_{1.2}Mn_{0.54}Ni_{0.13}Co_{0.13}O_2$ pristine in line with the sol-gel procedure adopted from Srivastava et al.[31] Briefly, stoichiometric amounts of the nitrate salt precursors were dissolved in deionized water. The solution was continuously stirred and nitric acid was introduced into the solution to give the final molar ratio of transitional metal ions to nitric acid of 2:1. Ammonium hydroxide (NH_4OH) solution was used to adjust the pH to 9.0. The solution was stirred for a further 3 h at 80 °C to obtain a clear solution. The clear solution was evaporated in an oven at 120 °C, and the dry gel was calcined for 12 h at 900 °C, to obtain the $Li_{1.2}Mn_{0.54}Ni_{0.13}Co_{0.13}O_2$ cathode material. Hereafter the uncoated material is referred to as the pristine. To prepare the Al_2O_3-coated sample, the pristine $Li_{1.2}Mn_{0.54}Ni_{0.13}Co_{0.13}O_2$ cathode material was ground into a fine powder and dispersed in deionized water under continuous stirring. Aluminium isopropoxide, $C_9H_{21}O_3Al$ (98.8%), was then added as the Al^{3+} precursor. The resulting suspension was stirred for 3 h at 80 °C to facilitate the deposition of the Al^{3+} onto the surface of the cathode particles. The product was subsequently dried, ground into a fine powder using a mortar and pestle, and calcined at 850 °C for 10 h to obtain the Al_2O_3-coated $Li_{1.2}Mn_{0.54}Ni_{0.13}Co_{0.13}O_2$ cathode material. The as-synthesized pristine and coated samples were characterized using X-ray diffraction (XRD), scanning electron microscopy coupled with energy-dispersive X-ray spectroscopy (SEM-EDS), Raman spectroscopy, and electrochemical testing to evaluate the influence of the coating on the performance and cycling stability of the cathode material.

Material Characterization

The X-ray diffraction analysis, Rigaku Ultima IV powder X-Ray Diffractometer equipped with a Cu Kα radiation of λ = 1.5406 Å at the 2θ range of 10–90° was used to investigate the crystal structure, expansion/contraction of the lattice parameters *a*, *b* and *c*, and formation of the spinel phase after prolonged cycling.[18] The lattice parameters and structural refinement analysis were determined by Rietveld refinement methods using FullProf Suite software packages. The surface and cross-sectional morphology, surface chemical composition, and elemental mapping of the pristine and Al_2O_3-coated samples were investigated using a Zeiss Supra 55 scanning electron microscope (SEM) with an accelerating voltage of 15 kV coupled with an energy-dispersive X-ray spectroscopy (EDS).

Battery fabrication and electrochemical measurement

Before electrochemical analysis, half-cells were fabricated using the following procedure. First, 80% Li/Mn-rich cathode active material was mixed with 10% wt polyvinylidene difluoride (PVDF) binder additive and 10% conductive carbon in an agate mortar. The ratios of the cathode material, conductive carbon, and PVDF, were optimized to establish the optimal loading for the cathode material.[32] The conductive carbon, PVDF, and cathode material were dispersed in N-methyl-2-pyrrolidine (NMP), and mixed to form a slurry. The slurry was then uniformly coated onto Al foil (current collector) with a thickness of 200 µm and allowed to dry in an oven at 60 °C. The dried slurry on Al foil was cut into discs and assembled into a coin cell using an air-stable Li anode,[33] a polypropylene seperator and 1 M $LiPF_6$ dissolved in a mixture of ethylene carbonate and dimethyl carbonate (EC/DMC) as the electrolyte. The coin cells of LIR 2032 type cells were assembled in an argon-filled glove box (MBraun, Germany).[32] The assembled coin cells were left for 24 hours to ensure complete electrolyte infiltration. Therefore, the voltage profiles, galvanostatic charge/discharge, and capacity retention tests were performed on the cathode materials pristine $Li_{1.2}Mn_{0.54}Ni_{0.13}Co_{0.13}O_2$ and Al_2O_3-coated $Li_{1.2}Mn_{0.54}Ni_{0.13}Co_{0.13}O_2$ at room temperature in the potential window of 2.8 to 4.35 V vs. Li/Li^+ characterization using a Maccor 4000 series battery tester.

RESULTS AND DISCUSSION

XRD, Raman Spectrum and SEM analysis

The XRD results of pristine $Li_{1.2}Mn_{0.54}Ni_{0.13}Co_{0.13}O_2$ and Al_2O_3-coated $Li_{1.2}Mn_{0.54}Ni_{0.13}Co_{0.13}O_2$ samples are depicted in Figure 1c. The diffraction patterns exhibit the characteristic structure of Li-rich Mn-based layered oxide materials, with the major diffraction peaks corresponding to a hexagonal structure with space group $R\bar{3}m$ layered component (ICDD 00-049-0524). The superlattice peaks observed at

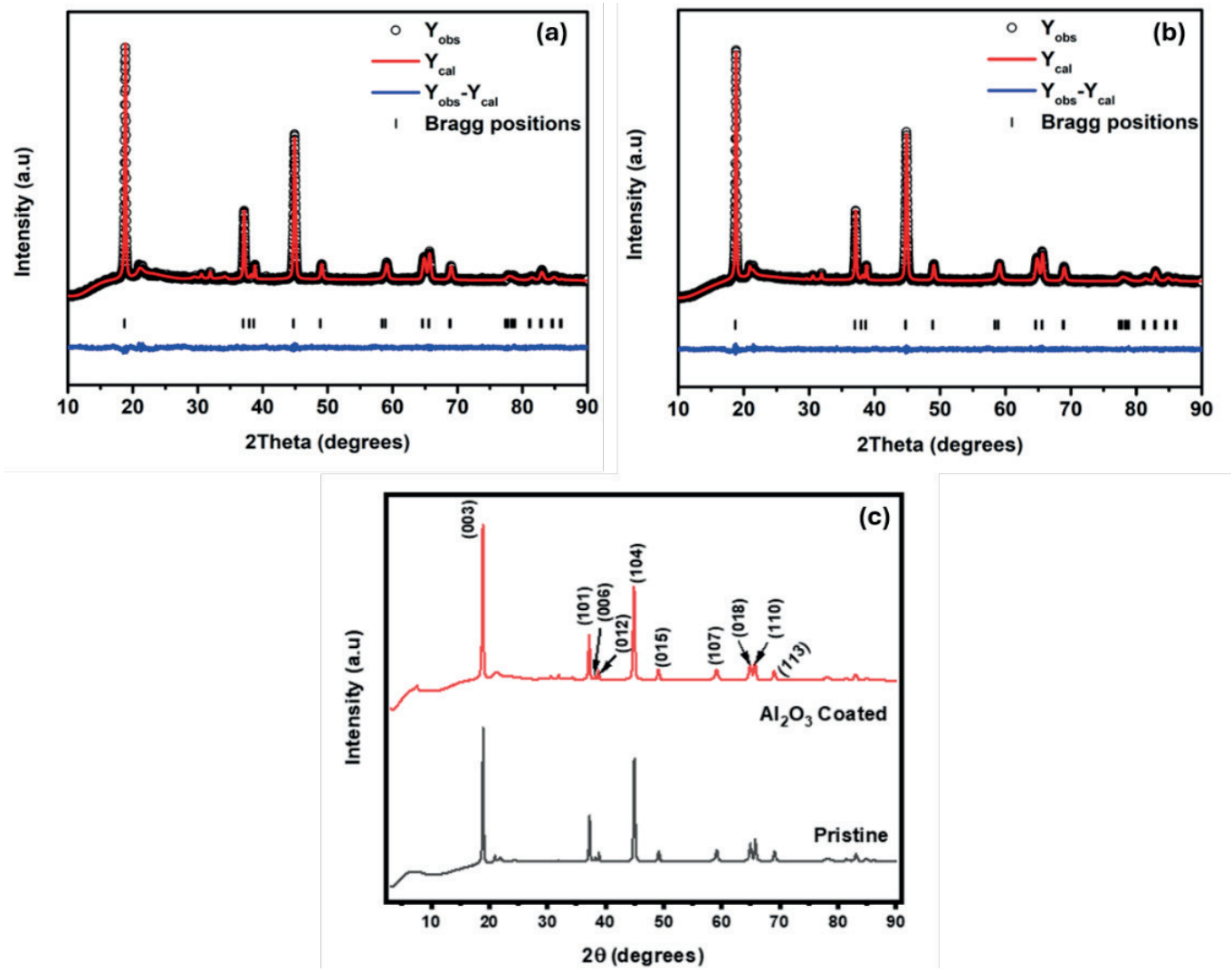


Figure 1: (a) Rietveld refinement profile of the pristine $Li_{1.2}Mn_{0.54}Ni_{0.13}Co_{0.13}O_2$, (b) Rietveld refinement profile of Al_2O_3-coated $Li_{1.2}Mn_{0.54}Ni_{0.13}Co_{0.13}O_2$ and (c) XRD pattern of the pristine and Al_2O_3-coated $Li_{1.2}Mn_{0.54}Ni_{0.13}Co_{0.13}O_2$.

20–22° 2θ confirm the existence of Li_2MnO_3 and can be indexed to the Li_2MnO_3 (JCPDS Card No. 27-1252) with monoclinic unit cell and space group C2/m.[34] The clear splitting of the peaks (006)/(012) and (108)/(110) indicates an ordered distribution of cations in the layered structure (see Figure 1(c)).

The weak reflections observed in the diffraction patterns were adequately indexed by the $R\bar{3}m$ structural model during Rietveld refinement, and no additional crystalline phase attributable to Al_2O_3 was identified.

Rietveld refinement was performed using the FullProf Suite for both the pristine and Al_2O_3-coated samples using the $R\bar{3}m$ structural model. The observed and calculated diffraction profiles, Bragg reflection positions, and difference profiles are presented in Figure 1(a) and (b), while the corresponding structural and refinement parameters are summarized in Table 1. The refinement yielded Rwp values of 7.56% and 9.19% for the pristine and Al_2O_3-coated samples, respectively, indicating reasonable agreement between the observed and calculated diffraction profiles. The pristine sample exhibited lattice parameters of a = b = 2.8763 Å and c = 14.2315 Å, while the Al_2O_3-coated sample exhibited a = b = 2.8733 Å and c = 14.235 Å. The corresponding unit-cell volumes were 101.432 and 101.735 Å^3, respectively. The c/a ratio changed only slightly from 4.948 for the pristine sample to 4.954 for the coated sample. The relatively small changes in the lattice parameters and unit-cell dimensions indicate that the characteristic layered framework was largely retained following the Al_2O_3 coating process.

Table 1: Structural and Rietveld refinement parameters of pristine and Al_2O_3-coated $Li_{1.2}Mn_{0.54}Ni_{0.13}Co_{0.13}O_2$.

Parameter	Pristine	Al_2O_3-coated
Space group	$R\bar{3}m$	$R\bar{3}m$
a = b (Å)	2.8763	2.8733
c (Å)	14.2315	14.235
Unit cell volume (Å^3)	101.432	101.735
c/a	4.948	4.954
$I_{(003)}/I_{(104)}$	1.38	1.46
Rp (%)	6.12	6.69
Rwp (%)	7.56	9.19
Rexp (%)	4.96	5.63
χ^2	2.32	2.66

Raman scattering spectra of the as-synthesized $Li_{1.2}Mn_{0.54}Ni_{0.13}Co_{0.13}O_2$ and Al_2O_3-coated $Li_{1.2}Mn_{0.54}Ni_{0.13}Co_{0.13}O_2$, depicted in Figure 2 confirms that the pristine and modified samples had similar Raman fingerprints, translating to near-identical crystalline structure, crystal phase, and chemical composition. The four Raman-active modes of $Li_{1.2}Ni_{0.13}Co_{0.13}Mn_{0.54}O_2$ are evident at 590, 471, 415, and 362 cm^{-1} with slight variations in the intensity of the

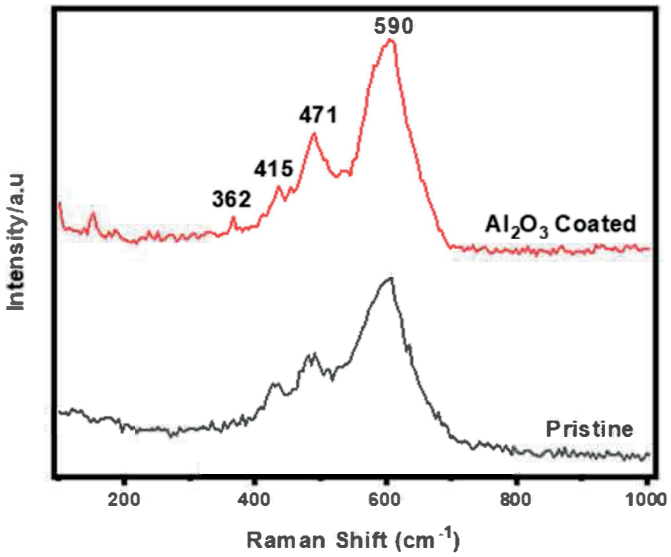


Figure 2: Raman spectra for the Al_2O_3 coated Li/Mn-rich cathode material and pristine

bands. The visible vibrational modes of the spectrum are assigned to the expected frequencies of C2/m (monoclinic) and R$\bar{3}$m (hexagonal) lattice symmetries. The two peaks at 471 and 590 cm^{-1} are assigned to O-M-O bending in plane and M-O stretching out of plane of the R$\bar{3}$m lattice.[35] The peaks at 362 and 415 cm^{-1} were attributed to the C2/m (monoclinic) phase.[36]

SEM micrographs confirm the synthesized materials exhibited a homogenous morphology with faceted and irregularly shaped agglomerated particles as observed in the micrographs in Figures 3(a) and 3(d) (circled in red). The hexagonal structures corroborate the XRD results. The micrographs also revealed interparticle voids between the irregularly shaped agglomerated particles (Figures 3a–f). These voids are expected to facilitate electrolyte penetration and improve contact between the electrolyte and the active material, thereby promoting lithium-ion transport during electrochemical cycling. In addition, the agglomerated morphology contributes to a relatively high surface area, which enhances the electrode-electrolyte interface.[37] The particles were observed to be predominantly submicron-sized and formed micrometre-scale agglomerates. The smooth appearance of some particles is attributed to the morphology of the synthesized powders, as the SEM characterization was performed

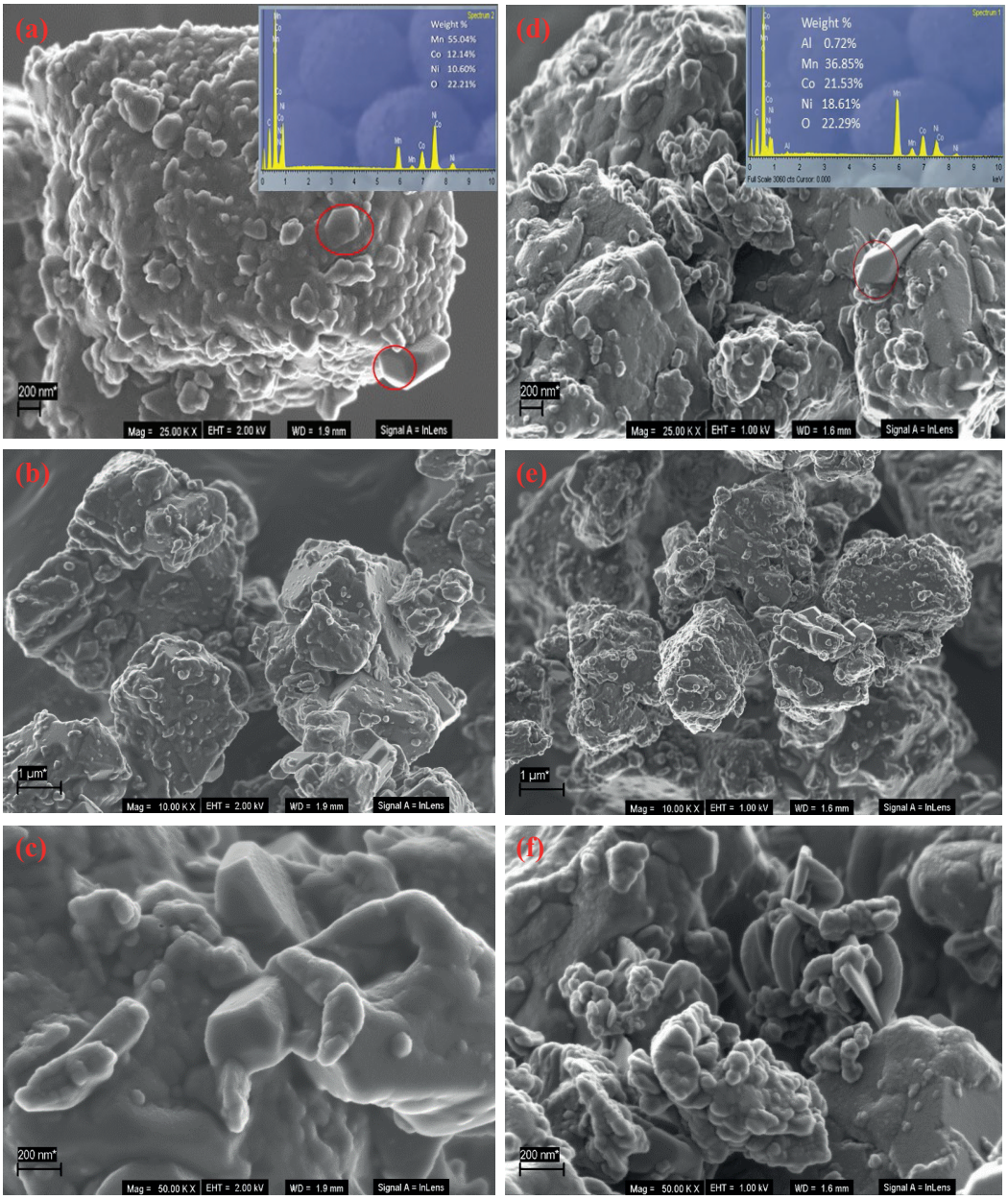


Figure 3: (a–c) SEM micrographs of the pristine $Li_{1.2}Mn_{0.54}Ni_{0.13}Co_{0.13}O_2$, (d–f) Al_2O_3-coated $Li_{1.2}Mn_{0.54}Ni_{0.13}Co_{0.13}O_2$. The EDS spectra for the pristine and modified samples are presented as an inset in Figures 3(a) and (d), respectively.

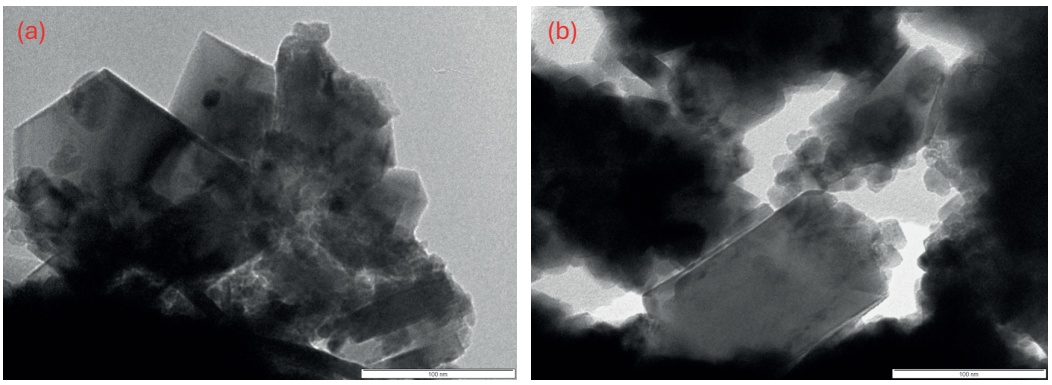


Figure 4: TEM micrographs of (a) pristine $Li_{1.2}Mn_{0.54}Ni_{0.13}Co_{0.13}O_2$ and (b) Al_2O_3-coated $Li_{1.2}Mn_{0.54}Ni_{0.13}Co_{0.13}O_2$ cathode materials.

prior to electrode fabrication; therefore, no binder was present during SEM analysis. The EDS spectra confirm the presence of transitional metals Mn, Co, and Ni in the pristine and Al_2O_3-coated samples (see Figure 3(a) and 3(d) inset). The transitional metals originate from the precursors used in the sol-gel synthesis. On a positive note, no extra peaks or impurities are detected from the EDS results; this confirms the absence of impurities from the sample, which is in line with the XRD data.

Figure 4(a) and (b) present the TEM micrographs of the pristine and Al_2O_3-coated $Li_{1.2}Mn_{0.54}Ni_{0.13}Co_{0.13}O_2$ samples, respectively. Both samples exhibit plate-like particles with well-defined facets, consistent with the morphology observed in the SEM micrographs. The Al_2O_3-coated sample retains a morphology similar to that of the pristine material, indicating that the surface coating process did not significantly alter the particle morphology. Slight contrast variations are observed near the particle surfaces of the coated sample, which may be associated with the presence of a thin surface-modified layer resulting from the Al_2O_3 coating process.

Electrochemical performance analysis

Figure 5 shows the analysis of the electrochemical performance of Mn-rich $Li_{1.2}Mn_{0.54}Ni_{0.13}Co_{0.13}O_2$ and Al_2O_3-coated $Li_{1.2}Mn_{0.54}Ni_{0.13}Co_{0.13}O_2$ samples. The charge-discharge profiles were recorded at a current density of 0.1 C within a voltage range of 2.8–4.35 V. The results reveal first-cycle discharge capacities of approximately 185 mAh g^{-1} for the pristine $Li_{1.2}Mn_{0.54}Ni_{0.13}Co_{0.13}O_2$ and 168 mAh g^{-1} for the Al_2O_3-coated $Li_{1.2}Mn_{0.54}Ni_{0.13}Co_{0.13}O_2$ sample. The discharge capacity of the coated sample shows the capacity value of 168 mAh g^{-1} for first cycle. The enhancement in the discharge capacity in the Al_2O_3 doped samples suggests that a small concentration of 1–3% of Al_2O_3 of the coating was critical to the enhancement of the electrochemical properties of the pristine; this is in line with past studies on the effectiveness of Al_2O_3 coating on Li/Mn-rich cathodes.[38]

The electrochemical performance of the pristine and the Al_2O_3-coated $Li_{1.2}Mn_{0.54}Ni_{0.13}Co_{0.13}O_2$ were investigated at 0.1 C via galvanostatic charge-discharge cycling, capacity retention, and voltage profiles. The higher capacity retention of 96% in the modified cathode and lesser voltage decay compared to the pristine, was an indication of slower layered to spinel phase transformation[39] and better cycling. The first and subsequent charge/discharge cycles of the pristine and the A_2O_3-coated samples at 0.1 C and 2.8–4.35V are presented in Figure 6. The long plateau in the high potential region 2.8–4.35V was attributed to the extraction of Li_2O from the Li_2MnO_3 (see Equation 1 in the introduction), accompanied by the diffusion of the transition metal (TM) ions from the surface to the bulk.[39] The migration of the TM ions confirms that surface coating does not change the structure of the core during cycling. The capacity retention of the pristine and Al_2O_3-coated materials and galvanostatic charge/discharge curves are depicted in Figures 6 at a current density of 0.1C within a voltage range of 2.6–4.5 V.

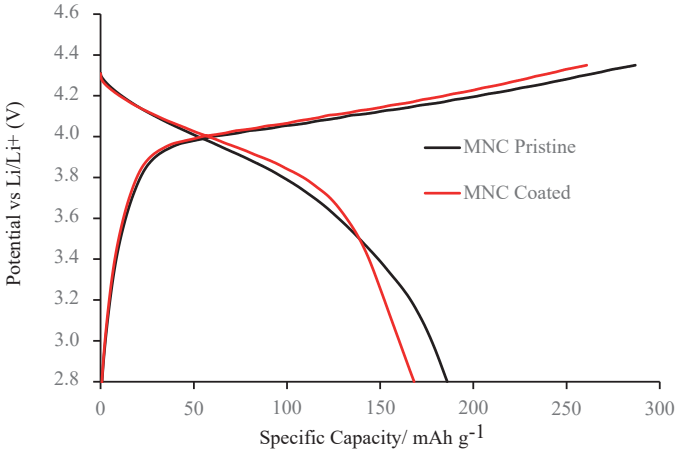


Figure 5: The first cycle charge-discharge curves of Pristine $Li_{1.2}Mn_{0.54}Ni_{0.13}Co_{0.13}O_2$ and Al_2O_3-coated $Li_{1.2}Mn_{0.54}Ni_{0.13}Co_{0.13}O_2$ cathodes at 0.1 C in potential window 2.8–4.35V.

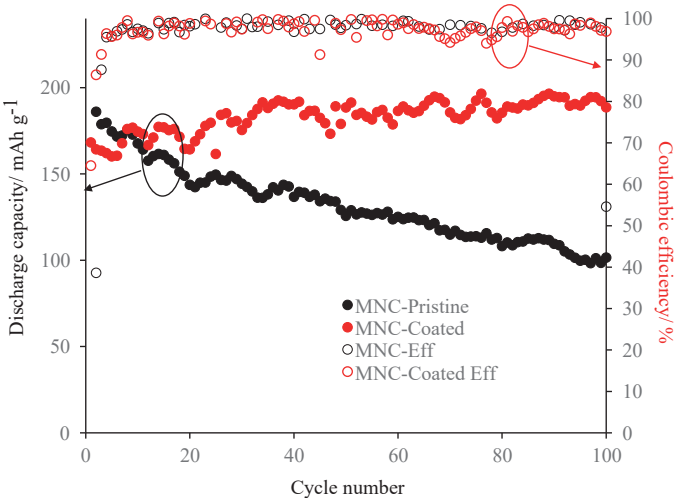


Figure 6: Cycle performance and Coulombic efficiency of pristine $Li_{1.2}Mn_{0.54}Ni_{0.13}Co_{0.13}O_2$ and Al_2O_3- coated $Li_{1.2}Mn_{0.54}Ni_{0.13}Co_{0.13}O_2$ at 0.1 C.

The cycling performance of $Li_{1.2}Mn_{0.54}Ni_{0.13}Co_{0.13}O_2$ and Al_2O_3-coated $Li_{1.2}Mn_{0.54}Ni_{0.13}Co_{0.13}O_2$ was carried out at 0.1 C rate in the voltage range of 2.8–4.35 V. Figure 6 shows the cycle number versus the discharge capacity for 100 cycles. The pristine maintained only 54% whereas the coated sample maintained stable cycling performance with a capacity retention of approximately 96% of their first cycle capacity after 100 cycles. Although the Al_2O_3 coating did not increase the discharge capacity, it contributed to reduced voltage decay, suggesting improved structural stability during repeated cycling. The as-synthesised pristine and Al_2O_3 coated materials in this

Table 2: Comparison of the capacity of this work and previous results.

Sample	Specific capacity (mAh g^{-1})	Capacity retention (%)	Potential window	Reference
Al_2O_3-coated $Li_{1.2}Mn_{0.54}Co_{0.13}Ni_{0.13}O_2$	175 (1 C)	70.28% (200 cycles)	2.0 – 4.8 V	[27]
Al_2O_3-coated $Li_{1.2}Mn_{0.54}Co_{0.13}Ni_{0.13}O_2$ nanotubes	259.74 (0.1 C)	78.3% (90 cycles)	2.0–4.5 V	[26]
$Li_{1.2}Mn_{0.54}Co_{0.13}Ni_{0.13}O_2$	189.5 (0.1 C)	66% (50 cycles)	2.0–4.8 V	[28]
$Li_{1.2}Mn_{0.54}Co_{0.13}Ni_{0.13}O_2$	210.5 (0.1 C)	42% (100 cycles)	2.0–4.8 V	[40]
$Li_{1.2}Mn_{0.54}Co_{0.13}Ni_{0.13}O_2$	185 (0.1 C)	54% (100 cycles)	2.8–4.35 V	This work
Al_2O_3-coated $Li_{1.2}Mn_{0.54}Co_{0.13}Ni_{0.13}O_2$	168 (0.1 C)	96% (100 cycles)	2.8–4.35 V	This work

work were compared and contrasted with other pristine and coated Li-rich MNCO cathode materials from the literature presented in Table 2. The specific discharge capacity delivered by this work were slightly low compared to the literatures, however the capacity retentions of the synthesised cathode materials high 96%. Compared with the previous works, our work displays a comparable performance within small potential window 2.8–4.35 V.

The incorporation of Al_2O_3 coating was expected to enhance the electrochemical performance by reducing capacity loss and protecting the electrode from electrolyte decomposition.[41] In the present study, the Al_2O_3-coated sample exhibited improved cycling stability but at a lower initial discharge capacity than the pristine material, indicating that the coating primarily contributed to surface protection rather than an increase in initial capacity. The claims made by Hu et al.[41] were corroborated by Shipper et al.[42] who suggested that Al^{3+} in the material had the potential to suppress HF attack and stabilize the layered crystal structure. Previous studies have proposed that the suppression of HF attack and stabilization of the cathode surface may involve the formation of $LiAlF_4$(s), $LiNiAlO_3$, and $LiAlO_2$(s) (see Equations 2a, b, and c) through reactions. However, these specific Al-containing phases were not directly identified by XRD in the present study and are therefore discussed only as possible reaction products based on the previously reported mechanisms.

$$Al^{3+} + Li^{+} + 4HF \rightarrow LiAlF_4(s)\downarrow + 4H^{+} \quad [2a]$$

$$Al^{3+} + Li^{+} + Ni^{2+} + 3H_2O \rightarrow LiNiAlO_3(s)\downarrow + 6H^{+} \quad [2b]$$

$$Al^{3+} + Li^{+} + 2H_2O \rightarrow LiAlO_2(s)\downarrow + 4H^{+} \quad [2c]$$

In line with the observations made by Shipper et al.[42] , Nayak et al.[43] noted that aluminum conferred both bulk and surface benefits as a result of partial substitution of Mn^{4+} with Al^{3+}. The substitution of partially charged ions increases the Ni^{3+} ratio, which is beneficial for charge compensation and mitigation of TM migration. The mitigation of TM migration helps prevent layered to spinel migration. Moreover, since the ionic radius of Ni^{3+} is lower than Ni^{2+} there is a decrease in cell parameters.[43] The observations from the present work are in partial agreement with these reports, particularly regarding the stabilizing role of the Al_2O_3 surface layer during cycling. However, the observations made by Shipper et al.,[42] and Nayak et al.[43] contrast with Hu et al.'s[41] study, which postulated that Al_2O_3's low ionic and electronic conductivity would impair discharge capacity; this would be prominent in materials prepared by sol-gel compared to atomic layer deposition (ALD), which enabled precise regulation of the coating thickness and uniformity. The lower initial discharge capacity observed in the present study is consistent with the explanation proposed by Hu et al., suggesting that the Al_2O_3 coating may introduce additional resistance to lithium-ion transport while still providing a protective surface layer.

CONCLUSION

This study investigated the effect of Al_2O_3 surface coating on the structural and electrochemical properties of Li-rich $Li_{1.2}Mn_{0.54}Ni_{0.13}Co_{0.13}O_2$ cathode materials synthesized using the sol-gel method. XRD, Raman spectroscopy, and SEM-EDS analyses confirmed the successful synthesis of the layered cathode material and the presence of the constituent elements without detectable impurities. Electrochemical evaluation showed that the Al_2O_3-coated cathode delivered an initial discharge capacity of 168 mAh g^{-1} at 0.1 C with a capacity retention of 96% after 100 cycles. Although the Al_2O_3 coating resulted in a lower initial discharge capacity than the pristine material, it is expected to suppress HF attack and improve the structural stability of the cathode during cycling. Overall, the findings demonstrate that Al_2O_3 surface modification is a promising approach for enhancing the long-term stability of Li-rich cathode materials for lithium-ion batteries. The discharge capacity of 168 mAh g^{-1} can be improved by optimizing the weight percentage of Al_2O_3 and the synthesis temperature.

SUPPLEMENTARY INFORMATION

There is no Supplementary Information for this article.

ACKNOWLEDGEMENTS

This study was supported by NRF grant for Competitive Programme for Rated Researchers (Grant No: 149610), Thuthuka (Grant No: TTK2205056950), SMU Electron Microscope Unit. and University of South Africa (UNISA).

AUTHOR CONTRIBUTIONS

All authors contributed to the study conception and design. Material preparation, data collection, and analysis were performed by SR, MRM, and MAK. The first draft of the manuscript was written by SR , JK and all authors commented on previous versions of the manuscript. This manuscript was guided by MRM and MAK. All authors read and approved the final manuscript.

DECLARATION OF COMPETING/FINANCIAL INTERESTS

The authors declare that they have no known competing financial interests or personal relationships that could have appeared to influence the work reported in this paper.

DECLARATION OF GENERATIVE AI AND AI-ASSISTED TECHNOLOGIES

The authors declare that no generative AI or AI-assisted technologies were used in the preparation of this manuscript.

AUTHOR ORCID IDS

Seipati Rasesemola: https://orcid.org/0000-0003-3998-760X
Rebecca Mhlongo: https://orcid.org/0000-0002-9096-4916
Mesfin A. Kebede: https://orcid.org/0000-0002-7764-0933

REFERENCES

1. Cui T, Li X, Fu Y. Characteristics, materials, and performance of Ru-containing oxide cathode materials for rechargeable batteries. eScience. 2024;4:100245. https://doi.org/10.1016/j.esci.2024.100245.
2. Jin Y, Zhao Z, Ren P, Zhang B, Chen Z, Guo Z, Ren F, Sun Z, Liu S, Song P, et al. Recent Advances in oxygen redox activity of lithium-rich manganese-based layered oxides cathode materials: mechanism, challenges

and strategies. Adv Energy Mater. 2024;14(40):2402061. https://doi.org/10.1002/aenm.202402061.

3. Kebede MA, Palaniyandy N, Koao LF. Layered, spinel, olivine, and silicate as cathode materials for lithium-ion battery In: Kebede MA, Ezema FI (editors), Electrochemical Devices for Energy Storage Applications. Boca Raton: CRC Press; 2019. pp. 1–17. https://doi.org/10.1201/9780367855116-1.
4. Zhu Y, Huang Y, Du R, Tang M, Wang B, Zhang J. Effect of Ni2 on Lithium-ion diffusion in layered LiNi1−x−yMnxCoyO2 materials. Crystals (Basel). 2021;11(5):465. https://doi.org/10.3390/cryst11050465.
5. Wei Y, Zheng J, Cui S, Song X, Su Y, Deng W, Wu Z, Wang X, Wang W, Rao M, et al. Kinetics tuning of Li-ion diffusion in layered Li(NixMnyCoz)O2. J Am Chem Soc. 2015;137(26):8364–8367. https://doi.org/10.1021/jacs.5b04040.
6. Kebede MA, Mhlongo MR, Rasesemola S, Sheha E, Makgopa K, Makgwane PR. Synthesis route effect on the electrochemical performance of LiNi0.6Mn0.2Co0.2O2 cathode materials for lithium ion battery. ChemistrySelect. 2025;10(34):e03335. https://doi.org/10.1002/slct.202503335.
7. Salgado RM, Danzi F, Oliveira JE, El-Azab A, Camanho PP, Braga MH. The latest trends in electric vehicles batteries. Molecules. 2021;26(11):3188. https://doi.org/10.3390/molecules26113188.
8. Luo J, Dai CY, Wang Z, Liu K, Mao WG, Fang DN, Chen X. In-situ measurements of mechanical and volume change of LiCoO2 lithium-ion batteries during repeated charge–discharge cycling by using digital image correlation. Measurement (Lond). 2016;94:759–770. https://doi.org/10.1016/j.measurement.2016.09.023.
9. Zhang W, Schröder D, Arlt T, Manke I, Koerver R, Pinedo R, Weber DA, Sann J, Zeier WG, Janek J. (Electro) chemical expansion during cycling: monitoring the pressure changes in operating solid-state lithium batteries. J Mater Chem A Mater Energy Sustain. 2017;5(20):9929–9936. https://doi.org/10.1039/C7TA02730C.
10. Vanaphuti P, Liu Y, Ma X, Fu J, Lin Y, Wen J, Yang Z, Wang Y. Stabilized lithium, manganese-rich layered cathode materials enabled by integrating Co-doping and nanocoating. ACS Appl Mater Interfaces. 2021;13(19):22597–22607. https://doi.org/10.1021/acsami.1c04718.
11. Wang L, Dai A, Xu W, Lee S, Cha W, Harder R, Liu T, Ren Y, Yin G, Zuo P, et al. Structural distortion induced by manganese activation in a lithium-rich layered cathode. J Am Chem Soc. 2020;142(35):14966–14973. https://doi.org/10.1021/jacs.0c05498.
12. Xie Y, Jin Y, Xiang L. Li-rich layered oxides: Structure, capacity and voltage fading mechanisms and solving strategies. Particuology. 2022;61:1–10. https://doi.org/10.1016/j.partic.2021.05.011.
13. Paulus A, Hendrickx M, Bercx M, Karakulina OM, Kirsanova MA, Lamoen D, Hadermann J, Abakumov AM, Van Bael MK, Hardy A. An in-depth study of Sn substitution in Li-rich/Mn-rich NMC as a cathode material for Li-ion batteries. Dalton Trans. 2020;49(30):10486–10497. https://doi.org/10.1039/D0DT01047B.
14. Zhao S, Yan K, Zhang J, Sun B, Wang G. Reaction mechanisms of layered lithium-rich cathode materials for high-energy lithium-ion batteries. Angew Chem Int Ed. 2021;60(5):2208–2220. https://doi.org/10.1002/anie.202000262.
15. Seo D, Lee J, Urban A, Malik R, Kang S, Ceder G. The structural and chemical origin of the oxygen redox activity in layered and cation-disordered Li-excess cathode materials. Nat Chem. 2016;8(7):692–697. https://doi.org/10.1038/nchem.2524.
16. Huang C, Fang Z, Wang Z, Zhao J, Zhao S, Ci L. Accelerating the activation of Li2MnO3 in Li-rich high-Mn cathodes to improve its electrochemical performance. Nanoscale. 2021;13(9):4921–4930. https://doi.org/10.1039/D0NR08980J.
17. Ates MN, Mukerjee S, Abraham KM. A high rate Li-rich layered MNC cathode material for lithium-ion batteries. RSC Adv. 2015;5(35):27375–27386. https://doi.org/10.1039/C4RA17235C.
18. Gu M, Belharouak I, Zheng J, Wu H, Xiao J, Genc A, Amine K, Thevuthasan S, Baer DR, Zhang J, et al. Formation of the spinel phase in the layered composite cathode used in Li-ion batteries. ACS Nano. 2013;7(1):760–767. https://doi.org/10.1021/nn305065u.
19. Farahmandjou M, Zhao S, Lai W, Sun B, Notten PH, Wang G. Oxygen redox chemistry in lithium-rich cathode materials for Li-ion batteries: understanding from atomic structure to nano-engineering. Nano Materials Science. 2022;4(4):322–338. https://doi.org/10.1016/j.nanoms.2022.03.004.
20. Kebede MA. An investigation of the lattice parameter and micro-strain behaviour of LiMn2O4 coated with LiMn1.5Ni0.5O4 to attain high-rate capability and cycling stability. J Energy Storage. 2023;72:108602. https://doi.org/10.1016/j.est.2023.108602.
21. Kebede MA, Ozoemena KI. Molten salt-directed synthesis method for LiMn2O4 nanorods as a cathode material for a lithium-ion battery with superior cyclability. Mater Res Express. 2017;4(2):025030. https://doi.org/10.1088/2053-1591/4/2/025030.
22. Chen W, Hsieh H, Wu D, Tang H, Chang-Liao K, Chi P, Wu PM, Wu M. Advanced TiO2/Al2O3 bilayer ALD coatings for improved lithium-rich layered oxide electrodes. ACS Appl Mater Interfaces. 2024;16(10):13029–13040. https://doi.org/10.1021/acsami.3c16948.
23. Zhao X, Liu Q, He W, Mu D, Li L, Chen R, Wu F. Uniform Al2O3 coating for improved cycling stability of O3-type sodium-ion batteries cathode: mechanisms and performance insights. J Energy Storage. 2025;131:117548. https://doi.org/10.1016/j.est.2025.117548.
24. Wang C, Tsai J, Lai T, Chang C. Investigation of structures and electrochemical performances of synergetic ZnO-Al2O3 nanolaminated coatings for Li-rich layered oxide cathodes. J Energy Storage. 2024;103:114331. https://doi.org/10.1016/j.est.2024.114331.
25. Liu Z, Zeng Y, Tan J, Wang H, Zhu Y, Geng X, Guttmann P, Hou X, Yang Y, Xu Y, et al. Revealing the degradation pathways of layered Li-rich oxide cathodes. Nat Nanotechnol. 2024;19(12):1821–1830. https://doi.org/10.1038/s41565-024-01773-4.
26. Chen Y, Wang X, Zhang J, Chen B, Xu J, Zhang S, Zhang L. 2O3-coated Li1.2Mn0.54Ni0.13Co0.13O2 nanotubes as cathode materials for high-performance lithium-ion batteries. RSC Adv. 2019;9(4):2172–2179. https://doi.org/10.1039/C8RA09428D.
27. Zhang Z, Lai X, Fan K, Liu S, Chai L, Zhu Z, Sun L, Zhou Z, Wang L, Hu Z, et al. Li1.2Ni0.13Co0.13Mn0.54O2 of Al2O3-coating cathode for high-performance lithium-ion batteries. Bull Mater Sci. 2024;47(3):165. https://doi.org/10.1007/s12034-024-03226-z.
28. Ma X, He H, Sun Y, Zhang Y. Synthesis of Li1.2Mn0.54Co0.13Ni0.13O2 by sol–gel method and its electrochemical properties as cathode materials for lithium-ion batteries. J Mater Sci Mater Electron. 2017;28(22):16665–16671. https://doi.org/10.1007/s10854-017-7578-y.
29. Zhang X, Belharouak I, Li L, Lei Y, Elam JW, Nie A, Chen X, Yassar RS, Axelbaum RL. Structural and electrochemical study of Al2O3 and TiO2 coated Li1.2Ni0.13Mn0.54Co0.13O2 cathode material using ALD. Adv Energy Mater. 2013;3(10):1299–1307. https://doi.org/10.1002/aenm.201300269.
30. Chen RL, Sayed FN, Banerjee H, Temprano I, Wan J, Morris AJ, Grey CP. Identification of the dual roles of Al2O3 coatings on NMC811-cathodes via theory and experiment. Energy Environ Sci. 2025;18(4):1879–1900. https://doi.org/10.1039/D4EE03444A.
31. Srivastava N, Singh SK, Meghnani D, Mishra R, Tiwari RK, Patel A, Tiwari A, Singh RK. Molybdenum-doped Li/Mn-rich layered transition metal oxide cathode material Li1.2Mn0.6Ni0.1Co0.1O2 with High Specific Capacity and Improved Cyclic Stability for Rechargeable Li-Batteries. ACS Appl Energy Mater. 2022;5(10):12183–12195. https://doi.org/10.1021/acsaem.2c01680.
32. Zhang H, Xu J, Zhang J. Surface-coated LiNi0. 8Co0. 1Mn0. 1O2 (NCM811) cathode materials by Al2O3, ZrO2, and Li2O-2B2O3 thin-layers for improving the performance of lithium ion batteries. Front Mater. 2019;6:309. https://doi.org/10.3389/fmats.2019.00309.
33. Shen X, Li Y, Qian T, Liu J, Zhou J, Yan C, Goodenough JB. Lithium anode stable in air for low-cost fabrication of a dendrite-free lithium battery. Nat Commun. 2019;10(1):900. https://doi.org/10.1038/s41467-019-08767-0.
34. Gu Y, Chen Y, Liu H, Wang Y, Wang C, Wu H. Structural characterization of layered LiNi0.85−xMnxCo0.15O2 with x= 0, 0.1, 0.2 and 0.4 oxide electrodes for Li batteries. J Alloys Compd. 2011;509(30):7915–7921. https://doi.org/10.1016/j.jallcom.2011.05.024.
35. Wang H, Hashem AM, Abdel-Ghany AE, Abbas SM, El-Tawil RS, Li T, Li X, El-Mounayri H, Tovar A, Zhu L, et al. Effect of cationic (Na+) and anionic (F−) co-doping on the structural and electrochemical properties of LiNi1/3Mn1/3Co1/3O2 cathode material for lithium-ion batteries. Int J Mol Sci. 2022;23(12):6755. https://doi.org/10.3390/ijms23126755.

36. Ruther RE, Callender AF, Zhou H, Martha SK, Nanda J. Raman microscopy of lithium-manganese-rich transition metal oxide cathodes. J Electrochem Soc. 2015;162(1):A98–A102. https://doi.org/10.1149/2.0361501jes.
37. Zhang Y, Zhang W, Shen S, Yan X, Wu A, Yin J, Zhang J. Hollow porous bowl-shaped lithium-rich cathode material for lithium-ion batteries with exceptional rate capability and stability. J Power Sources. 2018;380:164–173. https://doi.org/10.1016/j.jpowsour.2018.01.084.
38. Seteni B, Rapulenyane N, Ngila JC, Mpelane S, Luo H. Coating effect of LiFePO4 and Al2O3 on Li1.2Mn0.54Ni0.13Co0.13O2 cathode surface for lithium ion batteries. J Power Sources. 2017;353:210–220. https://doi.org/10.1016/j.jpowsour.2017.04.008.
39. Chen Q, Luo L, Wang L, Xie T, Dai S, Yang Y, Li Y, Yuan M. Enhanced electrochemical properties of Y2O3-coated-(lithium-manganese)-rich layered oxides as cathode materials for use in lithium-ion batteries. J Alloys Compd. 2018;735:1778–1786. https://doi.org/10.1016/j.jallcom.2017.11.362.
40. Yang S, Shao S, Xie Y. LiAlSiO4-coated Li1.2Mn0.54Ni0.13Co0.13O2 cathode: enhancing Li-ion battery performance. PLoS One. 2025;20(2):e0318327. https://doi.org/10.1371/journal.pone.0318327.
41. Hu D, Du F, Cao H, Zhou Q, Sun P, Xu T, Mei C, Hao Q, Fan Z, Zheng J. An effective strategy to control thickness of Al2O3 coating layer on nickel-rich cathode materials. J Electroanal Chem (Lausanne). 2021;880:114910. https://doi.org/10.1016/j.jelechem.2020.114910.
42. Schipper F, Nayak PK, Erickson EM, Amalraj SF, Srur-Lavi O, Penki TR, Talianker M, Grinblat J, Sclar H, Breuer O, et al. Study of cathode materials for lithium-ion batteries: recent progress and new challenges. Inorganics (Basel). 2017;5(2):32. https://doi.org/10.3390/inorganics5020032.
43. Nayak PK, Grinblat J, Levi M, Levi E, Kim S, Choi JW, Aurbach D. Al doping for mitigating the capacity fading and voltage decay of layered Li and Mn-rich cathodes for Li-Ion batteries. Adv Energy Mater. 2016;6(8):1502398. https://doi.org/10.1002/aenm.201502398.